1

Event Structure in the Production of High Mass Photon Pairs

J. Huston

Physics Department, Michigan State University, East Lansing, Michigan 48827

J.F. Owens

Physics Department, Florida State University, Tallahassee, Florida 32306-3016

(February 1, 2008)

Abstract

The event structure associated with the production of massive photon pairs is studied to $\mathcal{O}(\alpha^2 \alpha_s)$. The cross sections for two photon and two photon plus one jet events are given. The Dalitz plot structure of events with two photons and a jet is also presented. These distributions will provide checks on our understanding of the production mechanisms for massive photon pairs, a signal thought to be important for searches for the Higgs boson in the intermediate mass region.

Typeset using REVTEX

I. INTRODUCTION

The production of photons in high momentum transfer collisions is useful for a variety of reasons [1]. The single photon invariant cross section is one of several important sources of information on the gluon distribution through the role played by the subprocess $qg \to \gamma q$ [2]. The photon plus jet cross section may also provide additional constraints as the quantity of such data is increased. Photon pair production has already played a role in confirming the quark charge assignments and is one of many large momentum transfer processes used to check the QCD-based description of high-p_T scattering [3]. Most recently, photon pair production has received attention because of its role in the search for the Higgs boson in the intermediate mass region [4]. The signature provided by the decay $H \to \gamma\gamma$ is particularly clean, enabling one, in principle, to detect the relatively rare processes of Higgs production. However, a crucial element in this search is to understand the two-photon background that results from conventional scattering processes [5]. In addition, it has been suggested that the observation of the production of photon pairs may serve as a useful signal for new physics processes [6].

The purpose of this paper is to present predictions for the event structure in two photon events. In particular, we will focus on events with one additional jet in the final state. Such events can be conveniently analyzed in terms of several angular distributions and the structure of a two-dimensional Dalitz plot. In addition, the presence of the jet allows one to define three classes of events depending on whether the jet has the most, second most, or least transverse energy when compared to the two photons. A similar analysis has been proposed for events with one photon and two jets in the final state [7].

The plan of the paper is as follows. In Sec. II a brief description of the program will be given. In Sec. III the characteristics of the two photon plus jet final states will be presented for a set of cuts which could be appropriate for either the CDF or D0 experiments. Our summary and conclusions will be presented in Sec. IV.

II. $\mathcal{O}(\alpha^2 \alpha_S)$ CALCULATION

The program used for this analysis has been described in Ref. [8], so only a brief summary will be presented here. To order $\mathcal{O}(\alpha^2)$ the production of photon pairs proceeds via $q\bar{q} \to \gamma\gamma$. In addition, there are contributions from final states with a single photon and a jet where the jet gives rise to a photon. This is estimated by including the $q\bar{q} \to \gamma g$ and $qg \to \gamma q$ subprocesses convoluted with the appropriate photon fragmentation function. The latter is formally of $\mathcal{O}(\alpha/\alpha_s)$ which yields an overall factor of α^2 when combined with the factor of $\alpha\alpha_s$ coming from the subprocess. Similarly, one can have final states with two jets, each of which fragments to a photon plus hadrons. This contribution is given by the sum of all $2 \to 2$ parton-parton scattering subprocesses convoluted with two fragmentation functions. These last two contributions are referred to as single and double bremsstrahlung processes, respectively. Although formally of $\mathcal{O}(\alpha^2\alpha_s^2)$, one can also have significant contributions from the subprocess $gg \to \gamma\gamma$ at high energies where small values of x become important since the gluon distribution is large enough there to compensate for the suppression from the running coupling.

The $\mathcal{O}(\alpha^2\alpha_s)$ next-to-leading-logarithm calculation includes contributions from the one-loop corrections to $q\bar{q} \to \gamma\gamma$ and the $2 \to 3$ subprocesses $q\bar{q} \to \gamma\gamma g$ and $qg \to \gamma\gamma q$. The actual calculation is performed using a combination of Monte Carlo and analytic integration techniques. The regions of phase space corresponding to soft or collinear singularities are isolated by the use of cutoffs, δ_s and δ_c, applied to the Mandelstam variables for the $2 \to 3$ subprocesses. The squared matrix elements are integrated over the singular regions using dimensional regularization. The soft singularities cancel with corresponding terms from the one-loop corrections. Finally, the collinear singularities are factorized using the $\overline{\text{MS}}$ scheme and absorbed into the corresponding distribution or fragmentation function. All remaining integrations are performed via Monte Carlo. When properly executed, the cutoff dependence in such a calculation cancels between the two-body and three-body contributions which is appropriate since the cutoffs merely serve to mark where one switches from a Monte Carlo

to an analytic integration technique. Additional details can be found in Ref. [8].

The calculation outlined here includes contributions from all $\mathcal{O}(\alpha^2 \alpha_s)$ subprocesses where the photons both are part of the hard scatter. There are also fragmentation contributions where the hard scattering process is calculated to $\mathcal{O}(\alpha_s^3)$ and two of the jets fragment to photons. These contributions have not been incorporated into the calculation. However, for collider energies isolation cuts are employed to help reduce the hadronic background to the photon signals. These isolation cuts greatly reduce the fragmentation contributions. Another point to remember is that this calculation is next-to-leading-order for observables involving the photon pairs. However, for the two photon plus jet final states only the $2 \to 3$ subprocesses contribute, so this represents a leading order calculation for that case. There are, for example, corrections from $2 \to 4$ subprocesses where one of the final jets is not detected. These contributions are beyond the scope of this calculation.

III. PREDICTIONS

Predictions for two photon and two photon plus jet final states were generated using the program described in the previous section. The CTEQ2M distributions [9] were used with the factorization and renormalization scales chosen to be the maximum E_T in each event. A minimum transverse momentum cut of 10 GeV is applied to the photons and the jet. In addition, the pseudorapidities of the two photons are required to satisfy $|\eta| \leq 1$ and that of the jet to satisfy $|\eta| \leq 3$. Both photons are required to be isolated, *i.e.*, to have less than 4 GeV of additional energy in a cone of radius $R = \sqrt{\Delta\eta^2 + \Delta\phi^2}$ of 0.7 centered on the photon direction. Effectively, this just requires the two photons and the jet to be separated by more than $\Delta R = 0.7$. Such a cut greatly reduces contributions from subprocesses involving photon fragmentation functions. In the experimental analysis the isolation cut also discriminates against jets fragmenting into a leading π^0 or η, and thus greatly decreases the background to the true two photon signal. These cuts are typical of what would be appropriate for an analysis by either the D0 or CDF groups.

5

In Fig. 1 the cross section is shown for two photon and two photon plus jet production as a function of the total transverse energy $(E_T^{\gamma\gamma})$ of the two photons. The photon and jet (if present) are subject to the cuts described above. The top curve shows the total cross section while the bottom curve shows the cross section with a jet satisfying the above cuts. The fraction of the cross section coming from events with a jet in the final state that satisfies these cuts varies from about 60% for $E_T^{\gamma\gamma} = 100$ GeV to about 30% at the upper end of the curve. This ratio is larger than might have been expected since the rapidity interval for the accompanying jet is much larger than that for the photons.

In Fig. 2 the fractions of the two photon plus jet cross section coming from the $q\bar{q}$ and qg subprocesses are shown versus the total transverse energy in the final state, denoted by ΣE_T. At low ΣE_T the qg subprocess dominates while the $q\bar{q}$ subprocess dominates at high ΣE_T values. This is primarily due to the relative sizes of the gluon and quark distributions at low and high values of x.

For those events with a jet in the final state, the fractions of the cross section are plotted in Fig. 3 according to whether the jet has the largest, second largest, or least E_T among the two photons and the jet. It is useful to classify the events in this manner since the jet is the one object distinguishable form the others. The photon was used in this manner in a similar analysis of photon plus two jet events in Ref. [7]. The results in this figure show that at high ΣE_T it is most likely that the jet will have less E_T than either of the photons, while at lower values it is more likely that the jet will have more E_T than one or both of the photons.

For events with two photons and a jet in the final state, four kinematic variables in addition to the three-body center-of-mass energy must be specified in order to determine the final state configuration. It is convenient to use scaled energy variables for two of these. In the parton-parton center-of-mass frame the energies of the final state particles can be labelled as E_3, E_4, and E_5 in decreasing order of energy. The energy fractions $x_i = 2E_i/E_{tot}$ can then be constructed, with $E_{tot} = E_3 + E_4 + E_5$. Hence, $x_3 + x_4 + x_5 = 2$. The variable x_3

6

satisfies $\frac{2}{3} \leq x_3 \leq 1$, where the lower limit corresponds to the symmetric "Mercedes Benz" configuration with all three $x_i's$ being equal. As x_3 tends towards one, the vectors of particle 4 and 5 become collinear and opposite to that of particle 3. The allowed range for x_4 is $0.5 \leq x_4 \leq 1$ where the lower limit corresponds to $x_4 = x_5$ with particle 4 and 5 being collinear while the upper limit corresponds to $x_5 = 0$ and $x_3 + x_4 = 1$. Only two of the $x_i's$ are independent; these will be taken to be x_3 and x_4. Two angles are needed to complete the description of the final state. In the parton-parton center-of-mass frame, let θ^* be the angle between the direction of the incoming proton and the direction of the jet or photon with energy E_3. The plane containing the beam and this jet or photon will be referred to as the scattering plane. The second angle is ψ which is the angle between the normal to the scattering plane and the normal to the plane containing the remaining jet or photons.

The main point of this analysis is that examination of various distributions in terms of these kinematic variables may provide useful information concerning the accuracy of the current QCD-based description of two photon production. For example, some lego plots of x_3 versus x_4 for events where the jet is the most energetic are shown in Fig. 4, 5, and 6. In these cases the two photons recoil against the jet. The p_T, η, and isolation cuts described above have been applied. In Fig. 4 a cut requiring the total E_T to be greater than 60 GeV has been applied. No obvious structure is visible. However, any structure is hidden because the total E_T cut is low with respect to the individual minimum E_T requirements. In Fig. 5 the cut on the total E_T has been raised to 200 GeV and in Fig. 6 to 400 GeV. As the minimum for the total E_T is raised an enhancement in the region $x_3, x_4 \rightarrow 1$ begins to appear, reflecting the existence of a pole in the matrix element at $x_3 = x_4 = 1$. In this region one of the photons becomes soft, *i.e.,* approaches the minimum E_T value of 10 GeV. For high values of the total E_T it is expected that the majority of events in this class would have a high E_T jet, a slightly less energetic photon, and a relatively soft second photon.

The lego plots for the case where the jet is the second most energetic show a similar structure. A related, but somewhat different, pattern emerges when the jet has less energy than either of the photons. For this configuration the jet and the photon with the least

energy of the pair recoil against the most energetic photon. Again, a strong pole structure becomes increasingly evident for progressively higher values of total E_T. However, as shown in Fig. 7, the shape of the emerging pole structure is somewhat broader in this case as compared to the case where the jet is the most energetic. This can be ascribed to the fact that the subprocess $qg \to \gamma\gamma q$ does not have a soft singularity when the quark energy goes to zero, but it does when one of the photon energies goes to zero. This can be further illustrated by comparing Fig. 8 and Fig. 9 which show the contributions to Fig. 7 from the $q\bar{q} \to \gamma\gamma g$ and $qg \to \gamma\gamma q$ subprocesses, respectively.

We have examined the $\cos(\theta^*)$ and ψ distributions for the three cases where the jet has the most, second most, or least energy with minimum total E_T cut of 200 GeV applied. The ψ distributions are essentially the same for all three cases while some minor differences are apparent in the $\cos(\theta^*)$ distributions. However, the exact shapes are rather cut dependent and so have not been shown. The appropriate distributions can easily be generated once the appropriate cuts have been specified.

Several two photon events have been observed by the CDF Collaboration with values of total E_T exceeding 400 GeV [10]. Two of the three events have a jet associated with the two photons. In one event the jet is the most energetic and for the other it is the least energetic. Based on the previous discussion one might expect that the photon or jet with the least energy might have an E_T value near the minimum allowed, *i.e.,* that the event would be in the region of the corresponding lego plot where the enhancement due to the pole occurs. Instead, the energies are closer than would have been anticipated. The unusual topologies of these events may simply be due to statistical fluctuations, but the continued presence of a large number of such events as the data sample grows could signal the need for additional sources of high mass photon pairs in the calculation.

8

IV. SUMMARY AND CONCLUSIONS

As preparations for the next generation of colliders continues, interest in the $\gamma\gamma$ channel has remained high since it can be used to search for the intermediate mass Higgs boson. It is, therefore, necessary to understand the conventional QCD production mechanisms for photon pairs in order to be able to provide reliable background estimates. The study of the event structure of two photon plus jet events using the distributions suggested in this paper may well provide useful tests of our understanding.

REFERENCES

[1] J.F. Owens, Rev. Mod. Phys. **59**, 465 (1987).

[2] J.F. Owens and W.-K. Tung, Annu. Rev. Nucl. Part. Sci. **42**, 291 (1992).

[3] E.L. Berger, E. Btaaten, and R.D. Field, Nucl. Phys. **B239**, 52 (1984).

[4] J.F. Gunion, G.L. Kane, and J. Wudka, Nucl. Phys. **B299**, 231 (1988).

[5] H. Baer and J.F. Owens, Phys. Lett. **B205**, 377 (1988).

[6] T. Rizzo, Phys. Rev. **D51**, 1064 (1995).

[7] S. Keller and J.F. Owens, Phys. Lett. **B269**, 445 (1991).

[8] B. Bailey, J. Ohnemus, and J.F. Owens, Phys. Rev. **D46** 2018, 1992.

[9] H.-l Lai *et al.*, Phys. Rev. **D51**, 4763 (1995).

[10] R. Blair *et al.* (the CDF Collaboration), Proceedings of the 10th Topical Workshop on Proton-Antiproton Collider Physics, Fermilab, May, 1995.

FIGURES

FIG. 1. The two photon cross section (upper curve) and the two photon plus jet cross section (lower curve) versus the total transverse energy of the two photons, $E_T^{\gamma\gamma}$, using the cuts discussed in the text.

FIG. 2. The fractions of the two photon plus jet cross section coming from the $q\bar{q}$(solid) and the qg subprocesses (dashed).

FIG. 3. The fractions of the two photon plus jet cross section where the jet has the highest (solid), second highest (dashed), or least (dotted) E_T.

FIG. 4. Lego plot of x_3 versus x_4 when the jet has the largest of the three E_T values and ΣE_T is required to be greater than 60 GeV.

FIG. 5. Lego plot of x_3 versus x_4 when the jet has the largest of the three E_T values and ΣE_T is required to be greater than 200 GeV.

FIG. 6. Lego plot of x_3 versus x_4 when the jet has the largest of the three E_T values and ΣE_T is required to be greater than 400 GeV.

FIG. 7. Lego plot of x_3 versus x_4 when the jet has the least of the three E_T values and ΣE_T is required to be greater than 400 GeV.

FIG. 8. The contribution to the plot in the previous figure from the $q\bar{q}$ initial state.

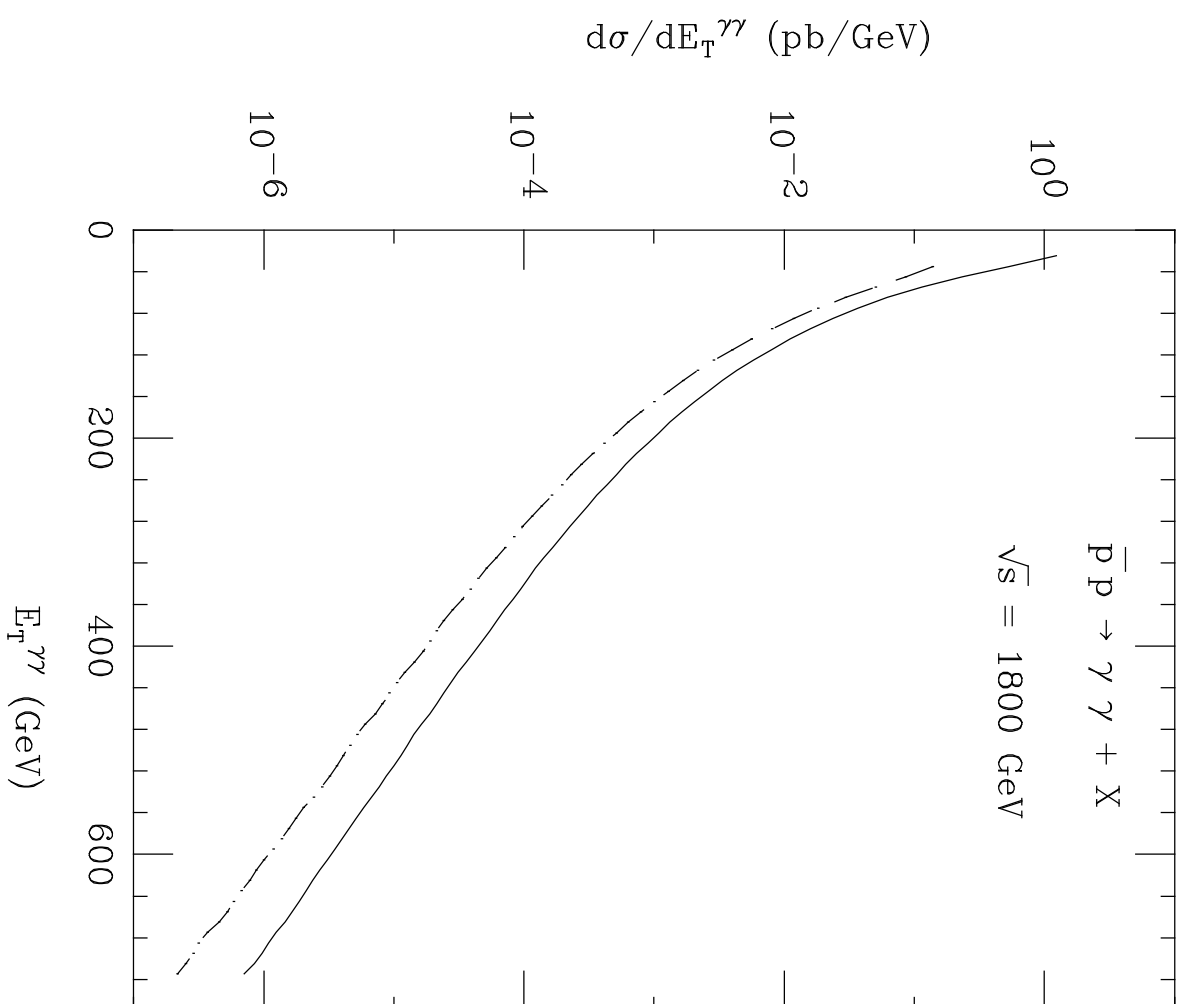FIG. 9. The same as the previous figure except for the qg initial state.
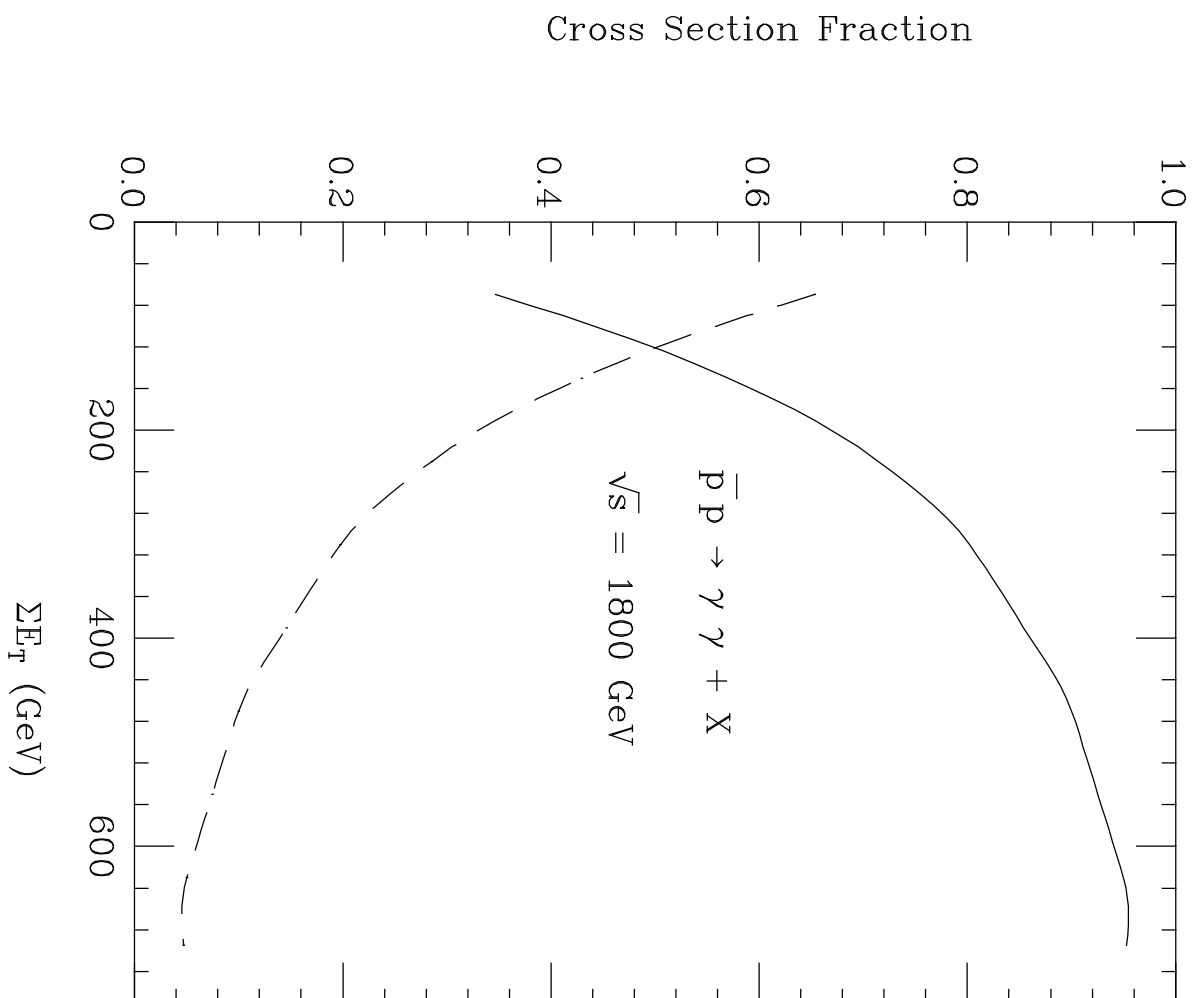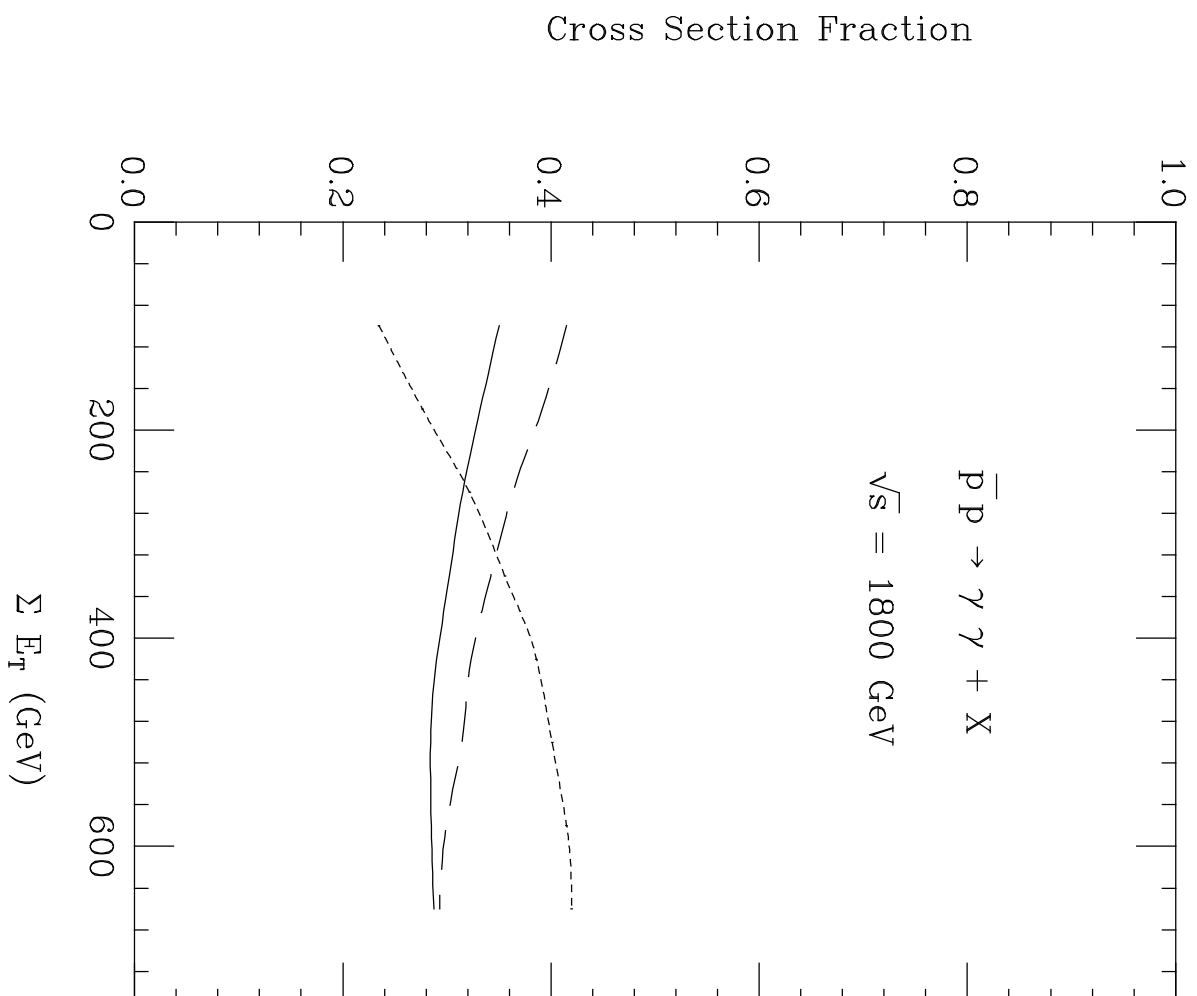
Figure 1

Cross Section Fraction

$\bar{p} p \to \gamma \gamma + X$

$\sqrt{s} = 1800$ GeV

ΣE_T (GeV)

Figure 2

Cross Section Fraction

$\bar{p}\, p \rightarrow \gamma\, \gamma + X$

$\sqrt{s} = 1800$ GeV

$\Sigma\ E_T$ (GeV)

Figure 3
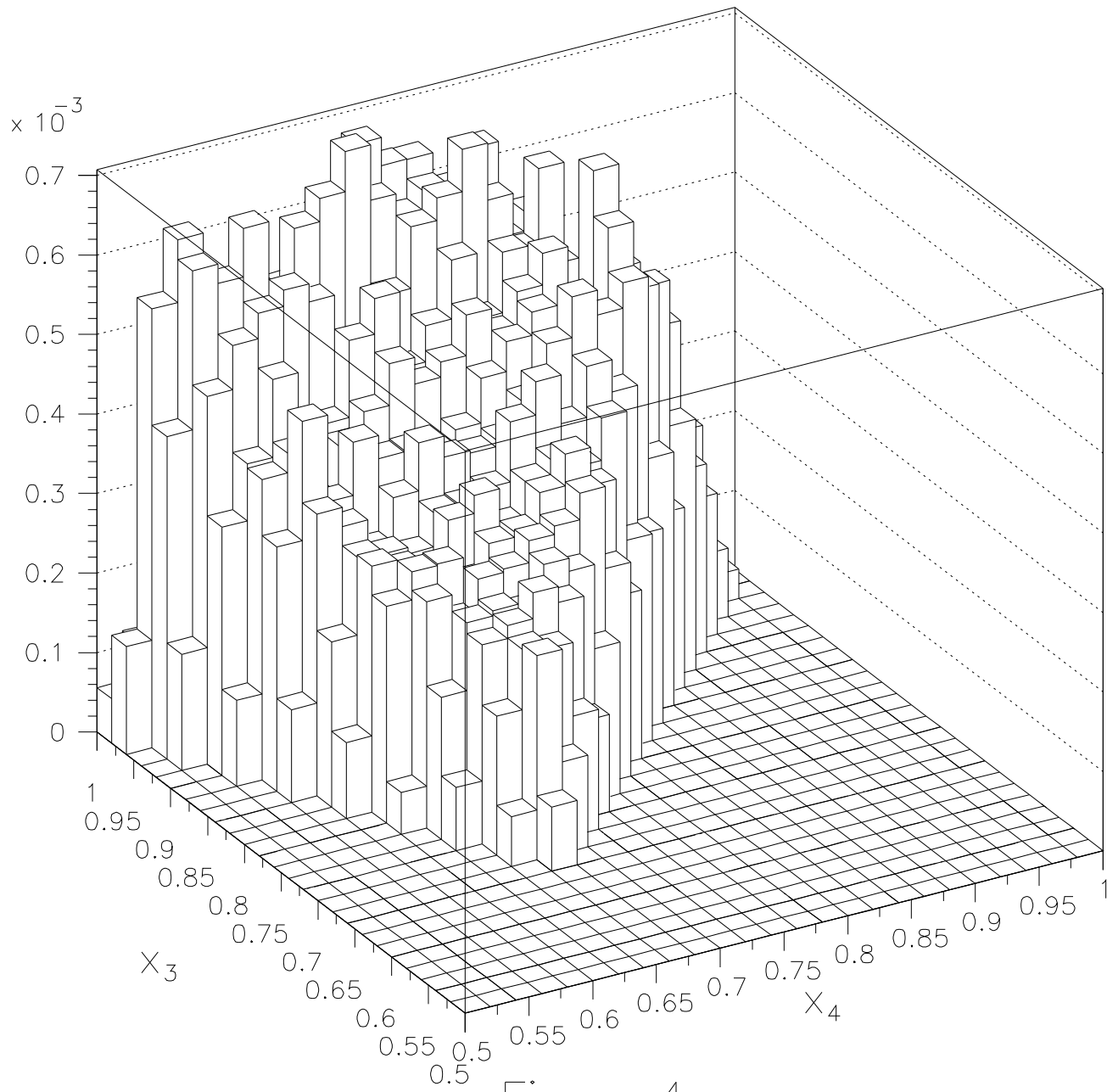
x_3 vs x_4 $(x_3 = jet)$

Figure 4

x_3 vs x_4 $(x_3 = jet)$
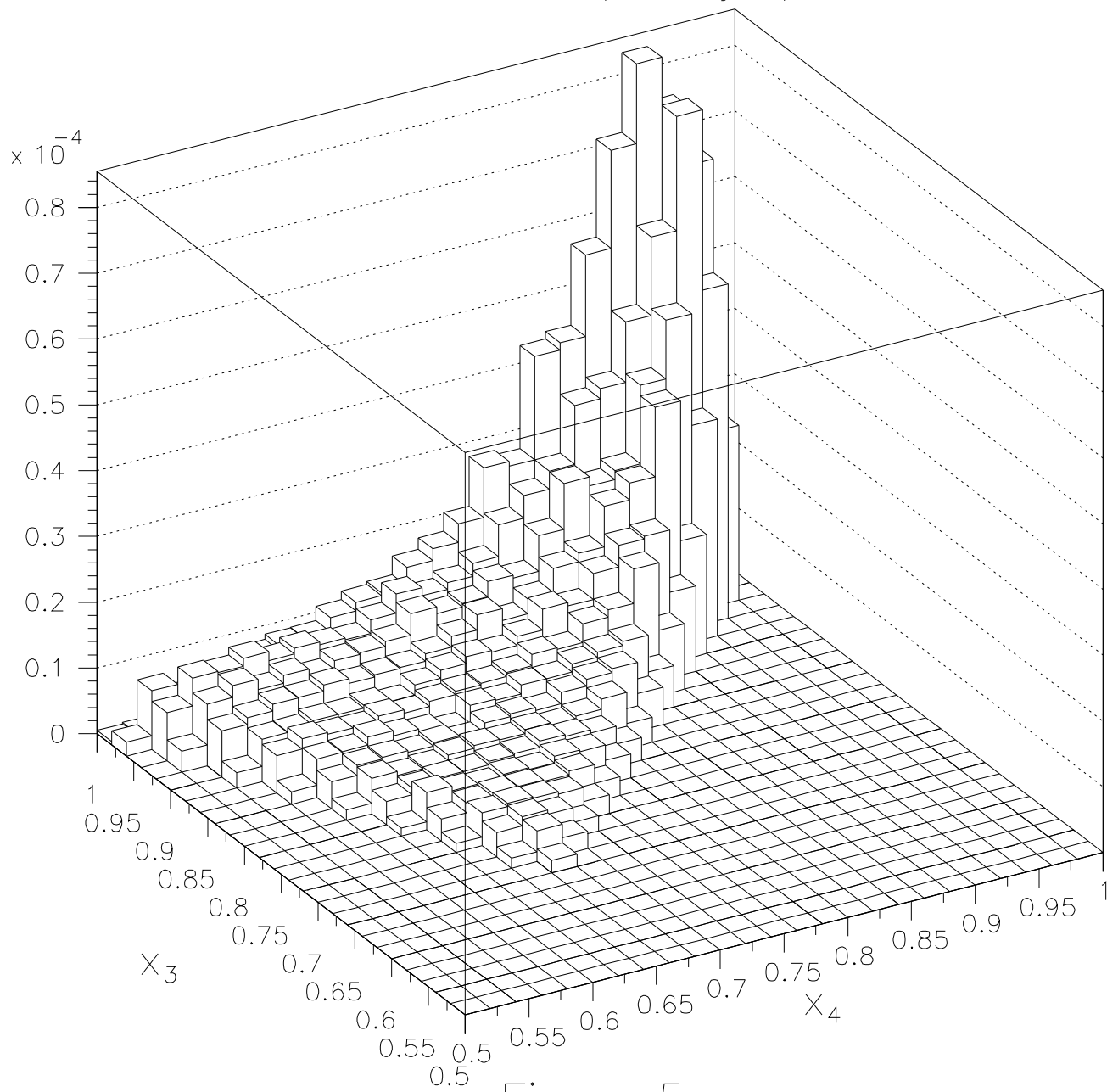
Figure 5

x_3 vs x_4 $(x_3 = jet)$

$\times 10^{-5}$

X_3

X_4
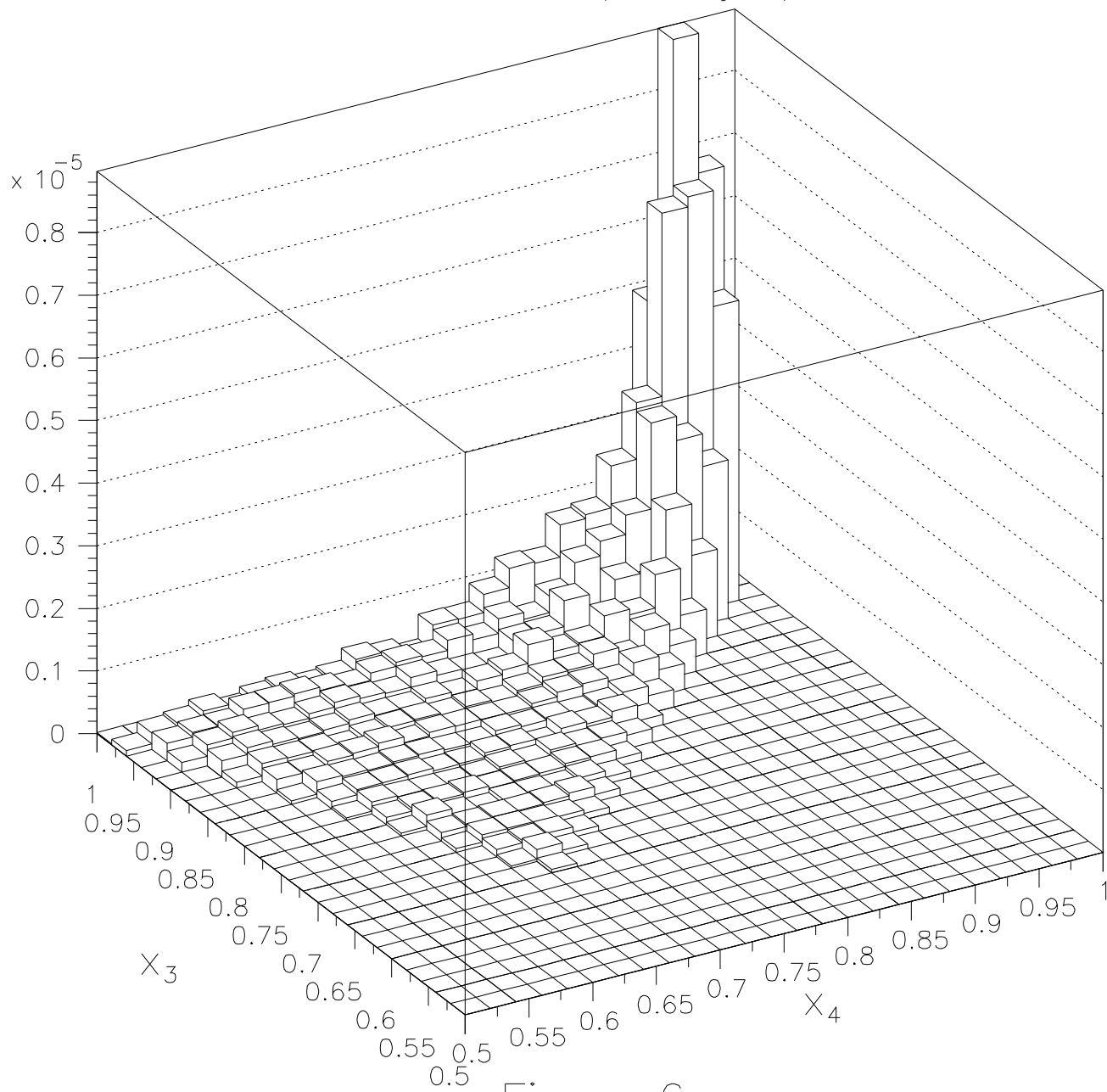
Figure 6

x_3 vs x_4 ($x_5 = $ jet)

$\times 10^{-5}$

X_3

X_4
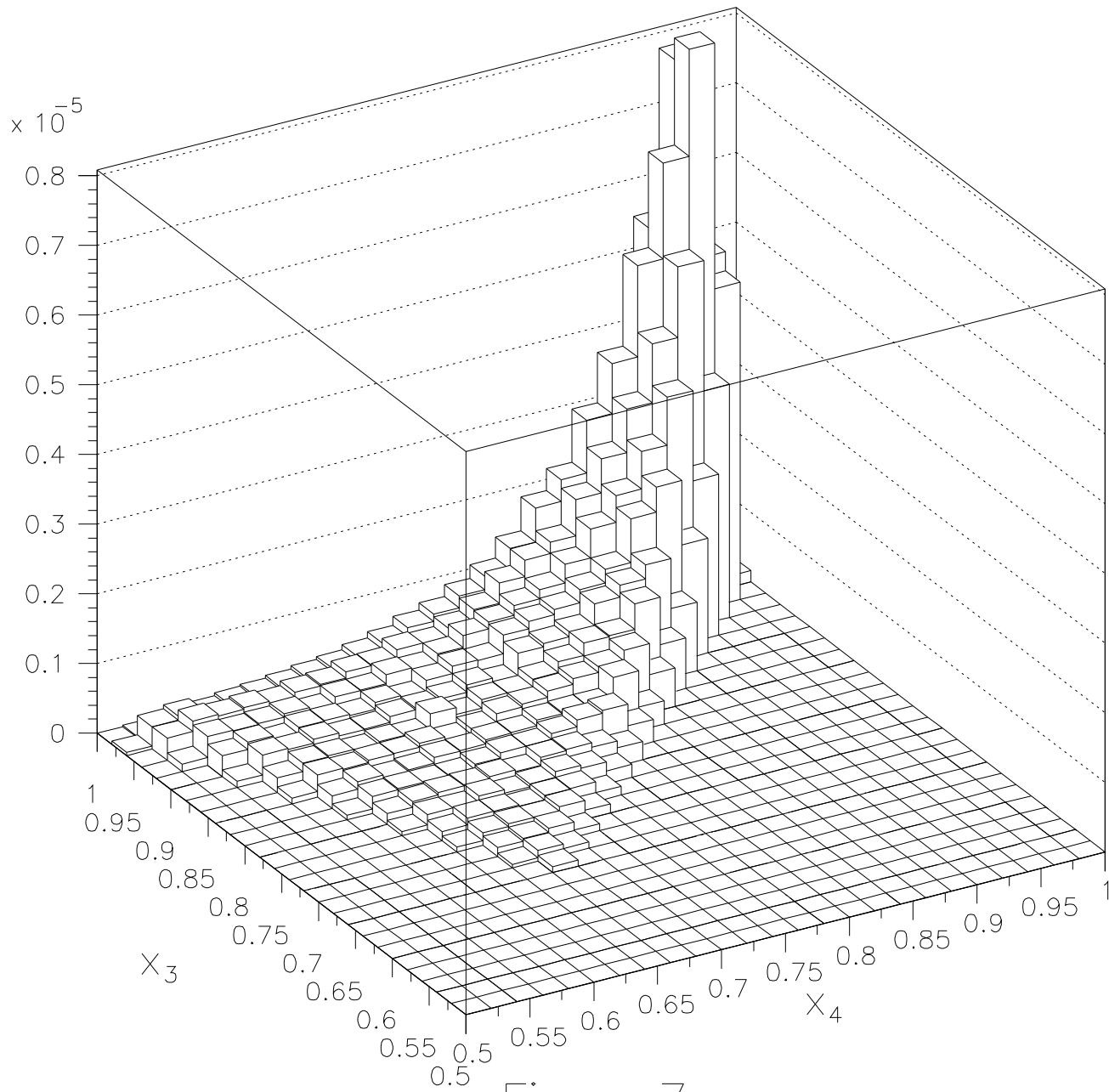
Figure 7

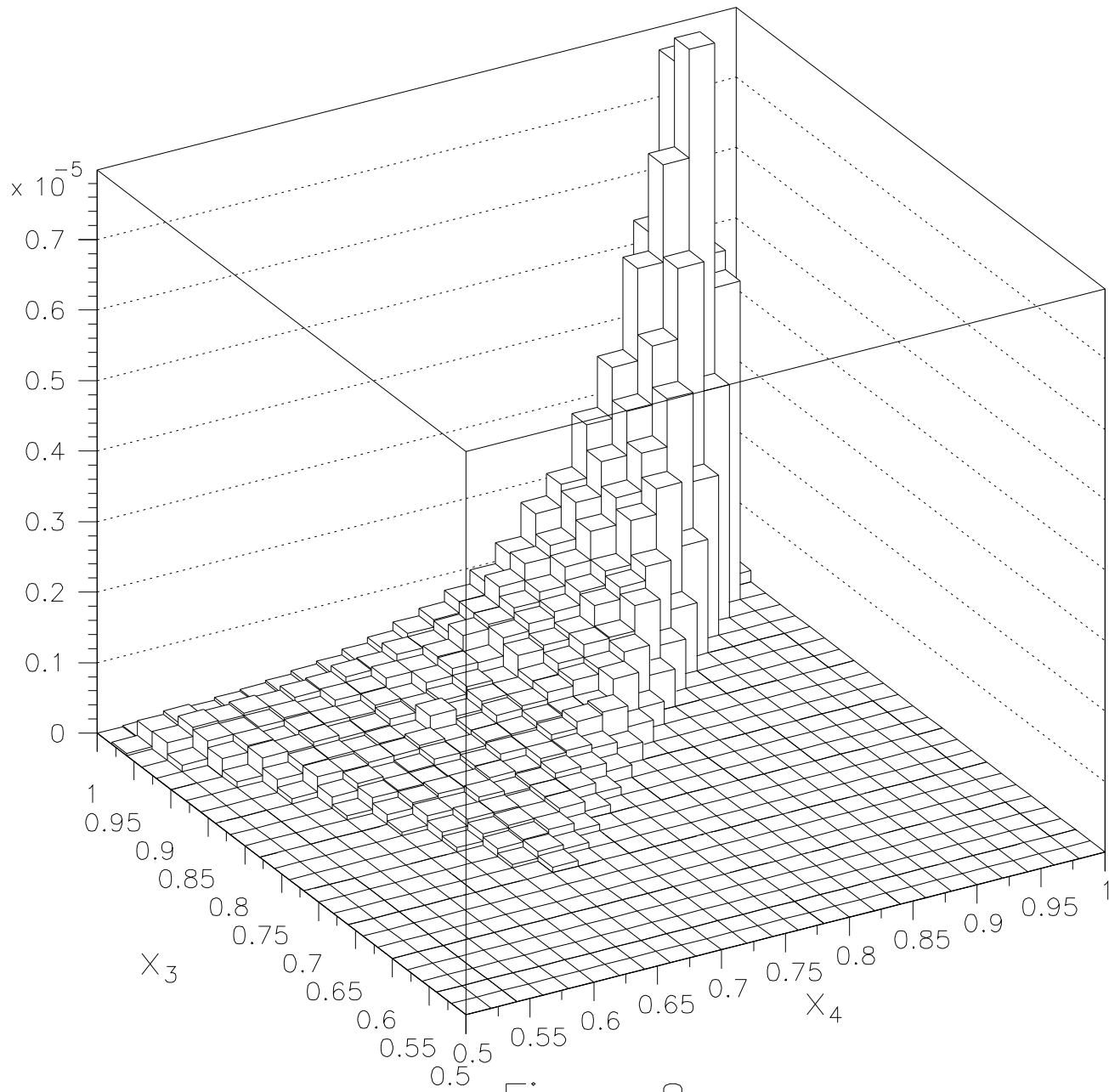x_3 vs x_4 $(x_5 = \text{jet} \quad q\bar{q} \text{ initial state})$
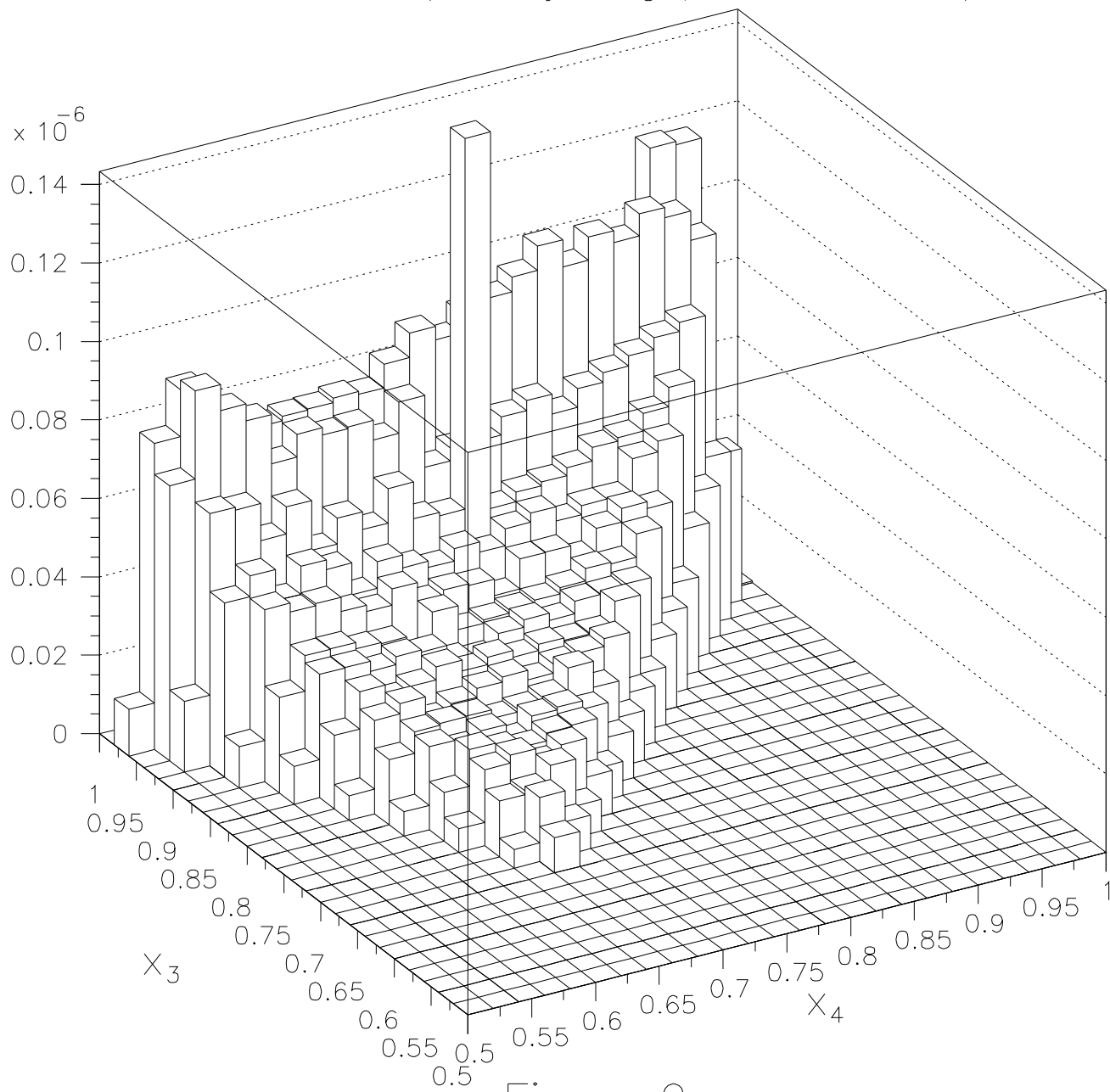
Figure 8

x_3 vs x_4 (x_5 = jet gq initial state)

Figure 9